Environmental Pollution 290 (2021) 118134

Contents lists available at ScienceDirect

Environmental Pollution

journal homepage: www.elsevier.com/locate/envpol

Efficacy of *in situ* active capping Cd highly contaminated sediments with nano-Fe_2O_3 modified biochar☆

Qunqun Liu [a,b], Yanqing Sheng [a,*], Xiaozhu Liu [a,b]

[a] Research Center for Coastal Environment Engineering Technology of Shandong Province, Yantai Institute of Coastal Zone Research, Chinese Academy of Sciences, Yantai, China
[b] University of Chinese Academy of Sciences, Beijing, China

ARTICLE INFO

Keywords:
Sediment
Cadmium (Cd)
Active *in situ* capping
Nano-Fe_2O_3
Biochar

ABSTRACT

Effective remediation of Cd polluted sediment is imperative for its potential damages to aquatic ecosystem. Biochar (BC) and nano-Fe_2O_3 modified BC (nFe_2O_3@BC) were conducted to remedy Cd highly contaminated sediments, and their performances, applicable conditions, and mechanisms were investigated. After 60 d capping, both BC and nFe_2O_3@BC capping inhibited Cd release from sediment to overlying water and pore-water (reduction rates >99%). The released Cd concentrations in overlying water with nFe_2O_3@BC capping decreased by 1.6–11.0 times compared to those of BC capping, indicating nFe_2O_3@BC presented a higher capping efficiency. Notably, the increases of acidity and disturbance intensity of overlying water weakened the capping efficiencies of nFe_2O_3@BC and BC. BC capping was inappropriate in acidic and neutral waters (pH 3, 5, and 7) because Cd maintained a continuous release after 15 d, while nFe_2O_3@BC capping was valid in all pH treatments. Under 150 rpm stirring treatment, Cd release rates with BC and nFe_2O_3@BC capping decreased after 15 d and 30 d, respectively. At 0 and 100 rpm treatments, Cd releases treated by nFe_2O_3@BC capping finally kept a balance, indicating nFe_2O_3@BC was valid at low disturbance intensity. BC and nFe_2O_3@BC capping inhibited Cd release via weakening the influences of pH and disturbance on sediment. However, capping layers should be further processed because most adsorbed Cd in capping layers (>98%) would be re-released into overlying water. Meanwhile, excessive application of nFe_2O_3@BC could increase the risk of Fe release. The results provide novel insights into the potential applications of nFe_2O_3@BC and BC *in situ* capping of Cd polluted sediments in field remediation.

1. Introduction

As the sink and source of heavy metals in water columns, sediment plays a key role in storing and transporting heavy metals in aquatic ecosystem (Wang et al., 2019). However, sediment heavy metal pollution has become a global environmental problem owing to vigorous development of metal smelting, electroplating, and mining, especially for Cd pollution (Wan et al., 2018; Xue et al., 2018). Previous studies reported sediments were highly contaminated by Cd with concentrations of 394 mg/kg in Jiehe River (China, Song et al., 2019) and 16,277 mg/kg in San Jorge River (Colombia, Marrugo-Negrete et al., 2021). Notably, Cd in sediment presents higher biotoxicity and mobility compared to other heavy metals (Liu et al., 2020a). The accumulated Cd in sediment would be re-released to overlying water with environment condition changes, thereby damaging the water quality and ecosystem balance; moreover, released Cd may accumulate into human body through food chain, exerting irreversible harms to human bone and kidney (Li et al., 2019a). Thus, effective remediation of Cd polluted sediment is imperative.

Generally, remediation of heavy metal polluted sediments includes *in situ* and *ex situ* techniques. *Ex situ* technique refers to traditional dredging. Nevertheless, dredging has some inherent drawbacks because disturbance may cause toxic substances re-release, posing harmful effects to aquatic organisms. Additionally, dredging also requires high cost, final disposal, and restoration for the benthic environment (Zhu et al., 2019). Conversely, *in situ* technique is relatively low cost, no secondary pollution, and without treatment of dredged sediment (Liu et al., 2020a). Among *in situ* techniques, *in situ* active capping has been

☆ This paper has been recommended for acceptance by Jörg Rinklebe.
* Corresponding author.
E-mail address: yqsheng@yic.ac.cn (Y. Sheng).

https://doi.org/10.1016/j.envpol.2021.118134
Received 12 April 2021; Received in revised form 2 September 2021; Accepted 6 September 2021
Available online 7 September 2021

considered a promising and effective technique for contaminated sediment remediation (Lin et al., 2020). It refers to apply active capping materials to cover the interface between sediment and overlying water to avoid pollutant re-release from polluted sediment (Lin et al., 2020).

The selection of active capping material is crucial in *in situ* active capping application. There are many capping materials, including zeolite (Xiong et al., 2018), industrial by-products (Taneez et al., 2018), modified attapulgite (Yin and Kong, 2015) and active carbon (Gu et al., 2017). Nevertheless, each capping material has its own disadvantages. As a pyrolysis product of agricultural waste, biochar (BC) can effectively reduce bioavailability of heavy metals, it has been widely applied to remedy heavy metal pollution due to its large specific surface area and abundant functional groups (El-Naggar et al., 2020). Accordingly, BC can be potentially applied in *in situ* remediation of Cd polluted sediment. Notably, its adsorption ability can be improved by iron-based material modification (Yang et al., 2018). Among many iron-based materials, Fe_2O_3 is low cost, natural abundance, and lower-toxicity (Liu et al., 2012). Meanwhile, chemical property of nano-Fe_2O_3 is more stable compared to nano-Fe^0 and nano-Fe_3O_4, and it can be easily obtained by industrial production (Li et al., 2019b). Generally, BC loaded by nano-Fe_2O_3 particles can restrict their aggregation and strengthen the reactivity of nano-Fe_2O_3, which will enhance adsorption capacity of Cd in aqueous solution compared to raw BC (Jin et al., 2011; Yuan et al., 2020). However, few studies concentrate on the remediation of Cd highly contaminated sediment using this high-efficiency adsorbent. Notably, changes in pH and hydraulic disturbance of overlying water always directly influence behavior and fate of heavy metals in sediment, because decrease of pH and/or increase of hydraulic disturbance may promote heavy metal release from sediment (Atkinson et al., 2007; Zhang et al., 2017). Consequently, durability and effectiveness of *in situ* active capping could be destroyed by pH and/or hydraulic disturbance changes. Nevertheless, research on this aspect is scarce, especially for the Cd, and the relevant mechanism is still unclear.

In this study, BC and nano-Fe_2O_3 modified BC (nFe_2O_3@BC) were used for *in situ* capping of Cd highly contaminated sediments to reduce the risk of Cd secondary release. The objectives are to (1) investigate the remediation effectiveness of BC and nFe_2O_3@BC on Cd highly polluted sediment; (2) evaluate the effects of pH and hydraulic disturbance on Cd release from sediment during remediation; and (3) explore the remediation mechanisms of BC and nFe_2O_3@BC for *in situ* capping Cd contaminated sediment. The results could provide new insights for the potential applications of BC and nFe_2O_3@BC in field remediation of Cd highly polluted sediment.

2. Materials and methods

2.1. Characterization and preparation of sediment

The surface sediment (0–10 cm) collected from Wulong River (Yantai, China) was performed for sediment remediation experiments. Sediment sample was naturally air-dried, ground, and sieved through 60 mesh (diameter 0.250 mm) for storage. The physicochemical properties and related determination methods of the sediment are provided in Table S1 and Text S1 in Supporting Information (SI), respectively. As shown in Table S1, the raw sediment pH was 8.05, and the electrical conductivity (EC) was 50.0 mS/cm. The total organic carbon (TOC) content was 0.52%, and the moisture content was 48.83%. The grain size of sediment was dominated by silt (66.75%), followed by sand, and clay. The Cd, Pb, Cu, and Zn concentrations (mg/kg) in sediment were 0.40, 31.32, 28.29, and 80.54, respectively. It found the Cd pollution in the raw sediment was relatively low. Therefore, for exploring the capping effects of BC and nFe_2O_3@BC on Cd highly contaminated sediment, additional Cd was added into raw sediment as artificially contaminated sediments, which could be used to investigate the remediation efficiency of Cd highly polluted sediments (Peng et al., 2020; Zhao et al., 2021). The additional Cd was added to the air-dried sediment based on the study of Zhao et al. (2021). Briefly, 9 g Cd $(NO_3)_2$ (purity: $\geq$ 99.0%) was dissolved in 16 L ultrapure water (18.25 MΩ*cm) and slowly added into 10 kg air-dried sediment. The sediment was intermittently stirred for 24 h to make it fully mixed, and then aged for 14 d. After natural air-drying, the Cd concentration in the aged sediment was up to 458.55 mg/kg. According to the previous studies (Song et al., 2019; Marrugo-Negrete et al., 2021), the aged sediment was reasonable for representing Cd highly contaminated sediment. Following the addition of Cd, the aged sediment was processed once again in a manner with the same as the raw sediment for further remediation experiments.

2.2. Preparation and characterization of remediation materials

The bamboo willow BC was prepared by pyrolysis of 5 min at 500 °C under oxygen-limited condition (Xiao et al., 2020). The prepared BC was oven-dried at 105 °C for 24 h, and then passed through 80 mesh (diameter 0.180 mm). The nFe_2O_3@BC was synthesized using the method of Li et al. (2019a, 2019b) with some modifications (SI Text 2), and the mass ratio of Fe to BC is 1:5. The pH values of BC and nFe_2O_3@BC were tested by 20 mL ultrapure water with 4 g BC and nFe_2O_3@BC severally. The pH of point zero charges (pH_{pzc}) of BC and nFe_2O_3@BC were analyzed using the titration method according to the method of Yu and Chen (2015). The maximum Cd adsorption capacities (Q_{max}) of BC and nFe_2O_3@BC were tested with Langmuir isotherm equation following the study of Huang et al. (2020). The cation exchange capacities (CEC) of BC and nFe_2O_3@BC were measured using Hexamminecobalt trichloride solution-Spectrophotometric method (MEPC, 2017). The elemental compositions of BC and nFe_2O_3@BC were analyzed by an element analyzer (Vario MACRO cube, Elementar, Germany). The ash contents were measured according to the method of Carbon materials – Determination of the ash content (AQSIQ and SAC, 2009). The Fe contents in BC and nFe_2O_3@BC were determined with the same as sediment Cd analysis (SI Text 1). The specific surface areas and pore volumes of BC and nFe_2O_3@BC were determined by an automatic surface analyzer (Quantachrome, USA). The mineral compositions of BC and nFe_2O_3@BC were tested by an X-ray diffractometer (XRD) with X-ray source of Cu-Ka radiation (Ultima IV, Japan). The surface morphology distribution was analyzed by a scanning electron microscopy (SEM, S-4800, Hitachi, Japan). The organic functional groups were measured using a Fourier transform infrared spectroscopy in the range of 4000–400 cm^{-1} (FTIR, Nicolet iS50, Thermo Fisher, USA). X-ray photoelectron spectroscopy (XPS) measurements were performed using a spectrometer (Thermo ESCALAB 250XI, USA) with an Al Kα X-ray as the excitation source.

2.3. Incubation experiment

The capping experiments were performed with six joint power-driven blenders followed some modifications (Zhang et al., 2017). Firstly, the 400 g prepared sediment (thickness: 5 cm; covering strength: 5.10 kg/m^2) was homogeneously paved in a 1000 mL high beaker (height: 20 cm; diameter: 10 cm), following by carefully adding 100 mL ultrapure water to infiltrate sediment; subsequently, 50 g BC or nFe_2O_3@BC (thickness: 1 cm; covering strength: 0.64 kg/m^2) was evenly spread on the sediment, and then 100 mL ultrapure water was slowly added; finally, 500 g analytically pure quartz sand (thickness: 1 cm; covering strength: 6.38 kg/m^2) was paved on the remediation materials to fix the capping layers, and 600 mL ultrapure water was slowly added (depth: 8 cm). The pH in overlying water was adjusted to 7 using 0.01 M HNO_3 and 0.01 M NaOH, and the stirring speed (SS) was set as 100 rpm to keep water turbulence and promote mass transfer. The overlying water pH values were measured and adjusted every 24 h. Meanwhile, all beakers were covered with plastic wrap to avoid dust and water evaporation. The treatment without BC and nFe_2O_3@BC capping layers was regarded as control. At predetermined time intervals (1, 3, 7,

15, 30, 45, and 60 d), 5 mL overlying water for all groups was sampled and acidified (pH < 2) to determine Cd and Fe by an ICP-MS (inductively coupled plasma mass spectrometer, ELAN DRC II, PerkinElmer, USA) and ICP-OES (inductively coupled plasma optical emission spectrometer, Optima 7000 DV, PerkinElmer, USA), respectively. Then, 5 mL ultrapure water was supplemented after every sampling to keep the volume of overlying water constant. The sampling of overlying water was conducted consistently in a same way and position during the entire capping experiments. In detail, the overlying water was sampled using a 5 mL pipettor (Eppendorf Research® plus, Germany), and the sampling position was 3 cm below the overlying water surface. Additionally, for studying pH influence, the experiments at pH 3, 5, and 9 were also conducted (Liu et al., 2021). Similarly, additional SSs were set as 0 and 150 rpm to explore the influence of disturbance intensities on BC and nFe_2O_3@BC capping. Three replicates were carried out for each group in the experiments.

2.4. Chemical analysis

After the capping, the overlying water and capping materials were carefully removed. Then, the incubated sediments with depths of 0–0.5 cm and 0.5–1.0 cm were collected to determine pH values and TOC contents in all treatments. The pH values and TOC contents in different sections of sediments were determined with the method of raw sediment analysis (SI Text 1). The porewaters in 0–0.5 cm and 0.5–1 cm sections of sediment were obtained via the centrifugation of wet sediment at 4000 rpm for 20 min, and the Cd concentration in porewater was analyzed using an ICP-MS. Moreover, for determining the stability of adsorbed Cd in capping layers, after the capping experiment, the capping layers were retrieved for analyzing the Cd fraction using a modified Bureau Communautaire de Référence (BCR) sequential extraction (Liu et al., 2020b). The detailed sequential extraction procedure is supplied in Table S2. The reduction efficiency of Cd in the overlying after capping was calculated as follows:

$$\text{Reduction efficiency } (\%) = \frac{C_{Ck} - C_{Cap}}{C_{Ck}} \quad (1)$$

where C_{Ck} and C_{Cap} are the Cd concentrations (μg/L) in the overlying water in the control and treated groups after capping, respectively.

2.5. DGT deployment and analysis

On 60 d capping, the Chelex DGT probes (Easysensor Ltd., China) were inserted into the sediments at pH 7 treatment. After 24 h, the Chelex DGT probes were taken out and washed thoroughly with ultrapure water. To ensure the continuity between different environmental media and the accuracy of the measurement, Chelex DGT probes were cut vertically into 5 mm slices. The measurement and calculation of the DGT-labile Cd concentrations in the overlying water-sediment profile was described as Chen et al. (2019). Briefly, each slice was placed in a 5 mL centrifuge tube, and added to 2 mL 1.0 M HNO_3 to extract the Cd; after 24 h, 1 mL extraction was diluted 10 times, and its Cd concentration was determined by an ICP-MS. The DGT-labile Cd concentration was calculated as follows:

$$C_{DGT} = \frac{M\Delta g}{DAT} \quad (2)$$

where M is the mass of Cd^{2+} adsorbed by DGT (μg); Δg is the thickness of diffusive layer (cm); A is the exposed area of ZrO-Chelex (cm^2); T is the measurement time of DGT device (s); and D is the diffusion coefficient of Cd in the diffusion film (5.55×10^{-6} cm^2/s) (Wang et al., 2016).

2.6. Statistical analysis

The significant difference of experimental data was analyzed by analysis of variance using SPSS version 19.0. The significant level was set as $P < 0.05$. Furthermore, homogeneity of variance of experimental data was measured with Bartlett's test.

3. Results and discussion

3.1. Characterization of BC and nFe_2O_3@BC

The XRD results of BC and nFe_2O_3@BC are presented in Fig. 1a. It found that XRD peaks assigned to hematite (Fe_2O_3, PDF-# 33–0664) occurred on the nFe_2O_3@BC pattern, while they were not observed in BC pattern. This indicated that nano-Fe_2O_3 was successfully loaded on raw BC surface. The SEM images of BC and nFe_2O_3@BC are shown in Fig. 1c and d, respectively. The BC surface was relatively smooth and many pore structures distributed on the BC surface, while the nFe_2O_3@BC surface was relatively rough. Many minute nano-particles existed on the surface of nFe_2O_3@BC, and their diameters ranged from 25 to 35 nm (Fig. S1). This could explain that Brunauer-Emmett-Teller (BET) specific surface area of nFe_2O_3@BC was higher than the BC (160.84 vs. 219.31 m^2/g, Table 1). FTIR analysis (Fig. 1b) showed BC and nFe_2O_3@BC had various oxygen-containing functional groups: –OH (3394 cm^{-1}), –COOH (2532 cm^{-1}), C═O (1582 cm^{-1}), phenolic–OH (1248 cm^{-1}) and C–O (1027 cm^{-1}), exhibiting they had potentially ability to complex divalent metal elements (such as Cd^{2+}) (El-Naggar et al., 2020; Liu et al., 2020a). Compared to the BC, the peak of Fe–O fall in the range of 600–500 cm^{-1} in nFe_2O_3@BC spectra (Yang et al., 2018), which also confirmed that nano-Fe_2O_3 was successfully loaded on BC surface.

As shown in Table 1, the pH of raw BC was 7.87, while the pH of nFe_2O_3@BC (7.37) was slightly lower. This was ascribed to the hydrolysis of Fe^{3+} from nano-Fe_2O_3 (Li et al., 2019a), and the hydrolysis process was as follows:

$$Fe^{3+} + 3H_2O \rightarrow Fe(OH)_3 + 3H^+ \quad (3)$$

Similarly, the pH_{pzc} of BC was also higher than that of nFe_2O_3@BC (9.55 vs. 8.12). The pore volume of nFe_2O_3@BC was larger than that of raw BC (0.093 vs. 0.183 cm^3/g) because calcination treatment during preparation process can enlarge the pore volume of nFe_2O_3@BC. After modification, the CEC of nFe_2O_3@BC was increased compared to raw BC because of Fe^{3+} release (Liu et al., 2021). Especially, the Q_{max} of nFe_2O_3@BC was 12.29 mg/g, which was 4.6 times higher than that of raw BC (2.68 mg/g), indicating Cd adsorption capacity of the nFe_2O_3@BC was greatly enhanced after modification. The elemental composition analysis showed raw BC was dominated by C (67.02%), H (3.92%), and O (12.84%). The mass proportions of C, H, and O in the nFe_2O_3@BC were decreased compared to raw BC because calcination would induce the loss of C, H, and O. On the contrary, the ash content in the nFe_2O_3@BC increased, this finding was coincided with the study of Ahmad et al. (2013), who found high temperature treatment could increase the ash content in BC. The Fe concentration in the nFe_2O_3@BC was much higher than that of raw BC owing to nano-Fe_2O_3 loading (7.91 vs. 178.51 g/kg).

3.2. The effects of capping on sediment properties

Sediment properties always regulate the behavior and mobility of heavy metals (Liu et al., 2020a). In this study, the TOC and pH of 0–0.5 cm and 0.5–1.0 cm sediments at all treatments were measured (Fig. 2). As shown in Fig. 2I, the TOC contents presented significant increases in the treated groups compared to the controls after capping ($P < 0.05$), confirming BC and nFe_2O_3@BC were successfully infiltrated into sediments. The TOC contents in 0–0.5 cm section at all treatments were higher than those in 0.5–1.0 cm section, indicating TOC decreased with increase of sediment depth. The infiltration of BC and nFe_2O_3@BC would be favorable to sediment remediation because they reduced the porosity of surface sediment, which restrained the release flux of

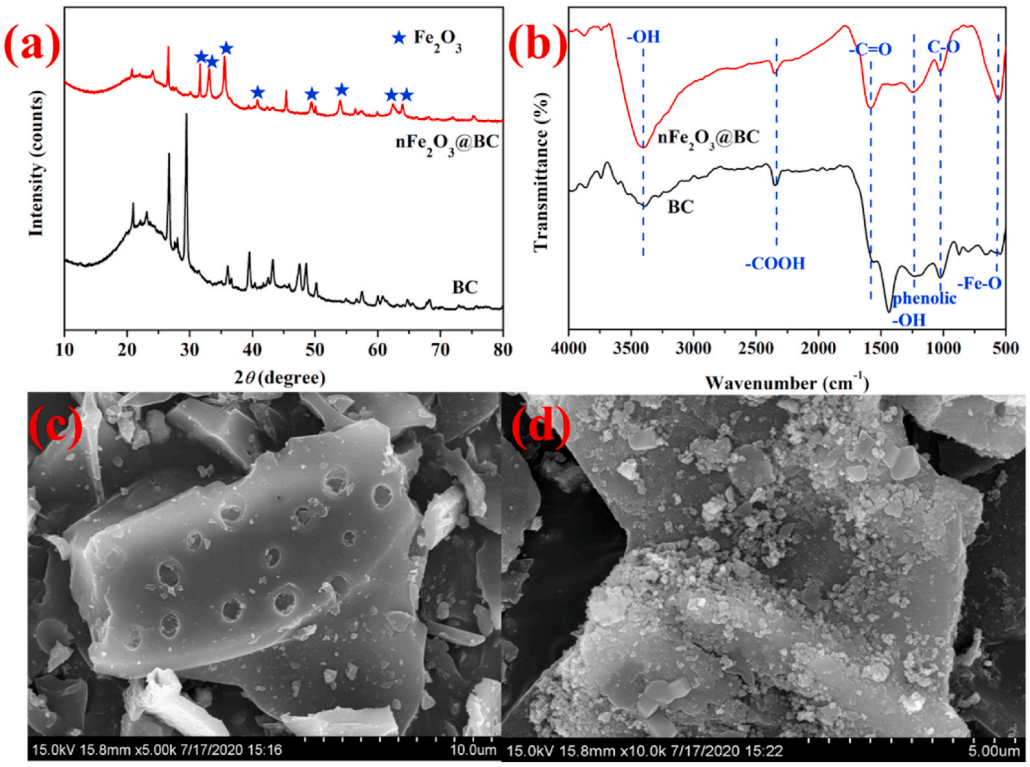

Fig. 1. XRD (a), FTIR spectrum (b) and SEM-EDS images (c, d) of BC and nFe_2O_3@BC

Table 1
The physicochemical properties of BC and nFe_2O_3@BC

Material	pH	pH_{pzc}	BET (m^2/g)	Pore volume (cm^3/g)	CEC (cmol/kg)	Q_{max}[a] (mg/g)	Fe (g/kg)	Ash (Mass ratio, %)	Elemental composition (Mass ratio, %)				
									C	H	O	N	S
BC	7.87 ±0.08	9.55 ±0.26	160.84 ± 20.96	0.093 ±0.018	21.51 ±0.58	2.68 ±0.19	9.71 ±0.18	15.14 ±2.13	67.02 ±5.01	3.92 ± 0.61	12.84 ± 1.64	0.74 ± 0.04	0.34 ± 0.04
nFe_2O_3@BC	7.37 ±0.03	8.12 ±0.17	219.31 ± 23.19	0.183 ±0.007	30.51 ±2.75	12.29 ±0.67	178.51 ±5.61	41.25 ±4.87	46.05 ±3.10	2.85 ± 0.15	8.93 ± 1.92	0.66 ± 0.12	0.25 ± 0.01

Note: Q_{max}[a]: pH = 7, 20 °C.

pollutants from sediment to overlying water (Zhu et al., 2019). Notably, the infiltration of remediation materials to sediment could produce some biological effects. According to a previous study (Liu et al., 2020a), the application of BC and nano-Fe^0 modified BC (nZVI/BC) enhanced the richness and diversity of sediment bacterial community. However, excessive application of BC and nZVI/BC lowered the richness and diversity of sediment bacterial community (Liu et al., 2021). Furthermore, benthic macrofauna function was impaired in sediment after 4 years of capping with activated carbon in the Grenland fjords, Norway (Raymond et al., 2021). Nevertheless, lanthanum-modified bentonite capping temporarily increased the bacterial community diversity in the bottom sediment due to capping created a new type of microenvironment across sediment-water interface (Yin et al., 2021). Obviously, different remediation materials associate various biological effects during contaminated sediment remediations. Hence, further researches about potential side-effects of the BC and nFe_2O_3@BC left in real conditions should be conducted.

At pH 3 and 5 treatments, sediment pH values in most treated groups were significantly higher than those in the controls ($P < 0.05$, Fig. 2II), suggesting sediment with BC and nFe_2O_3@BC capping was slightly influenced by low pH overlying water. It could be explained that buffering capacity of BC and nFe_2O_3@BC against H^+ was greater than that of quartz sand in the control. At pH 7 treatment, the sediment pH in the control nearly remained unchanged compared to treated groups ($P >$ 0.05). Instead, the pH in the control at pH 9 treatment was higher than those in the treated groups, and significant decreases were observed in nFe_2O_3@BC capping ($P < 0.05$), exhibiting an opposite trend compared to pH 3 and 5 treatments. This was because OH^- from overlying water to sediment was blocked by BC and nFe_2O_3@BC capping layers. Additionally, the pH values in 0–0.5 cm section with pH 3, 5 and 7 treatments were lower than those in 0.5–1.0 cm section, while the opposite result was observed in pH 9 treatment. It was due to that the upper sediment was easily influenced by pH change of overlying water. Similarly, the sediment pH values at different SS treatments were also various (Fig. 2IIc, e, and f), this was attributed to different disturbance intensities exerted different effects on the release of alkaline ions from sediments (such as OH^-, CO_3^{2-}, and HCO_3^-). Notably, the sediment pH values with nFe_2O_3@BC capping were lower than those of BC capping in most treatments, especially for pH 3 (0.5–1.0 cm) and 5 (0–0.5 cm) treatments ($P < 0.05$). This was probably caused by the hydrolysis of the dissolved Fe^{3+} from nFe_2O_3@BC as mentioned in Eq. (3). Moreover, the nano-Fe_2O_3 surface would be covered with Fe–OH groups in sediment, and generate H^+ through the complexation of Fe–OH groups with other metal ions, declining the sediment pH (Li et al., 2019a). The slight decrease in pH could promote heavy metal release from sediment (Liu et al., 2021); besides, the protonation of nano-Fe_2O_3 surface at low pH environment was also against Cd stabilization (Zhang et al., 2016). This should be noted in the application of nFe_2O_3@BC to cover sediments *in*

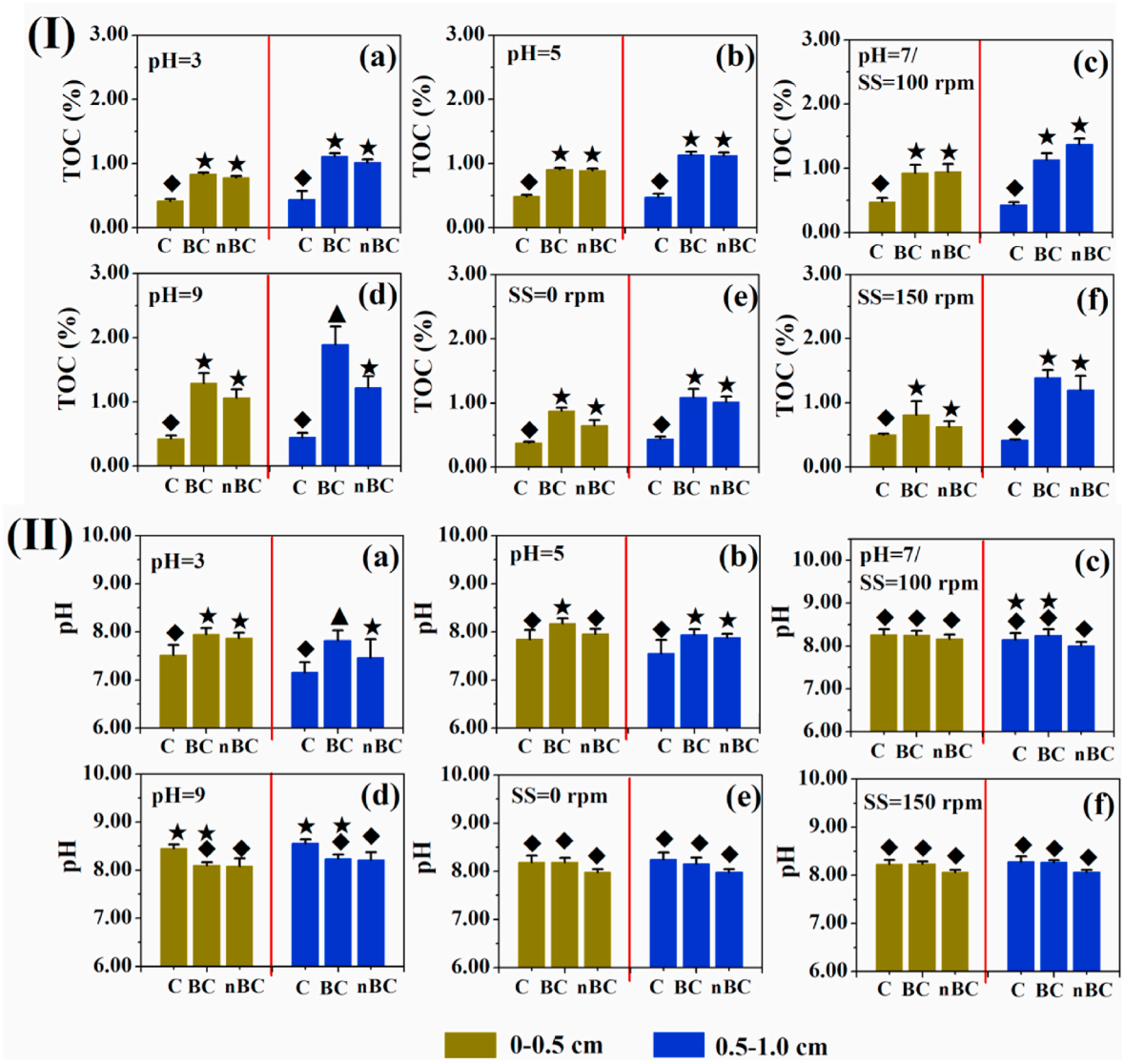

Fig. 2. The TOC contents (I) and pH values (II) of different depths of sediments in all groups (different symbols (◆, ★, and ▲) on the bars denote significant differences among different groups ($P < 0.05$); nBC represents nFe_2O_3@BC)

situ.

3.3. The effects of pH on Cd variations in overlying water and porewater

The pH of overlying water is closely related to environmental behavior of heavy metals in sediment (Zhang et al., 2017). The Cd variations in overlying water at different pH treatments are shown in Fig. 3. Overall, the Cd concentrations in overlying water increased with time during the capping process. At acid treatments (pH 3 and 5, Fig. 3a and b), although the Cd release patterns were similar to pH 7, their Cd concentrations presented huge differences. For the controls, Cd concentrations in overlying water at pH 3 and 5 treatments were 4.3 and 1.4 times higher than that in pH 7 treatment after capping, respectively. Nevertheless, the Cd at pH 9 treatment (Fig. 3d) was decreased by 23.7 times than that in pH 7. The main reason for these results was primarily owing to extensive H^+ could compete with Cd^{2+} for the sediment colloid, enhancing Cd release; furthermore, some original Cd precipitations (e.g. $CdCO_3$ and $Cd(OH)_2$) in sediment could be dissolved at low pH (Liu et al., 2021). By contrary, pH increase contributed to the formation of Cd precipitations, improving the stability of Cd in sediment (Liu et al., 2018a). Interestingly, the Cd variation in overlying water in the control at pH 9 treatment was greatly distinct from acid and neutral treatments, exhibiting a trend of increasing first (0–3 d), then decreasing (3–30 d), and finally flat (30–60 d). These phenomena indicated that dynamic processes of Cd migration and transformation existed in the sediment-overlying water system. At pH 9 treatment, Cd would be released into overlying water due to hydraulic disturbance, meanwhile, Cd in the overlying water always tends to migrate to the sediments by forming precipitations (Xue et al., 2018). Therefore, this phenomenon could be interpreted in the following process: the Cd firstly increased because its release rate was greater than the rate of precipitation; and then equilibrium reached, making Cd slightly fluctuant.

The Cd concentrations in overlying water with BC and nFe_2O_3@BC capping were significantly lower than those in the controls at all pH treatments ($P < 0.05$). It indicated BC and nFe_2O_3@BC capping significantly inhibited the Cd release (reduction rate >99%, Fig. S2), which was due to BC and nFe_2O_3@BC could effectively adsorb dissolved Cd^{2+}. Furthermore, capping materials could prevent dissolved oxygen entering the sediment, causing a strongly reducing condition in treated sediment. As reported by Yang et al. (2021), SO_4^{2-} in sediments could be reduced to sulfde (S^{2-}) under reducing condition, and the formed S^{2-} may react with Cd^{2+} to form insoluble sulfide precipitate (CdS), thereby inhibiting the release of Cd from sediment. With BC capping, the Cd in overlying water (μg/L) demonstrated a decrease order of pH 3 (43.02) >

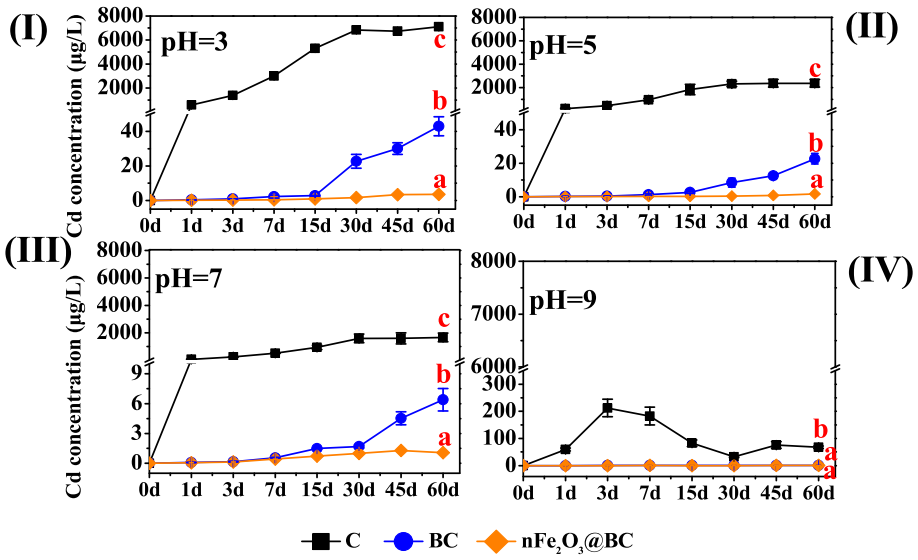

Fig. 3. Cd variations in overlying water under different pH treatments with time (different letters (a, b, and c) on the bars denote significant differences among different groups ($P < 0.05$); nBC represents nFe_2O_3@BC)

pH 5 (22.64)> pH 7 (6.38) > pH 9 (1.01), showing BC capping capacity weakened with pH decrease. This was attributed to that lots of H^+ in acidic environment would compete with metal ions for the active adsorption sites on the BC surface, and BC surface was positively charged, eventually reducing the adsorption capacity of BC for Cd^{2+} (Li et al., 2020). In neutral and alkaline treatments (pH 7 and 9), BC capping was more effective in inhibiting the release of Cd than that in acidic treatments. The BC surface was negatively charged at higher pH environment and presented stronger electrostatic affinity toward Cd^{2+}, accordingly enhancing its capping capacity (Xue et al., 2018). Additionally, the Cd release from sediment was inhibited in higher pH environment. Similar type of result was observed in nFe_2O_3@BC capping, and the Cd (μg/L) in overlying water were in the order of pH 3 (3.58) > pH 5 (1.77) > pH 7 (1.07) > pH 9 (0.39), decreasing by 11.0, 11.8, 5.0, and 1.6 times compared to those of BC capping, respectively. Obviously, the inhibitory effect of nFe_2O_3@BC on Cd release was superior to that of BC at all pH treatments. As mentioned in section 3.1, higher CEC of nFe_2O_3@BC could immobilize more dissolved Cd^{2+} via cation exchange compared to BC, meanwhile, higher specific surface area could provide more active adsorption sites to adsorb Cd^{2+} (Liu et al., 2020a). Additionally, nano-Fe_2O_3 loading could play a key role in strengthening Cd adsorption capacity of nFe_2O_3@BC.

In order to clarify the adsorption mechanism, XPS analysis was performed on nFe_2O_3@BC before and after Cd^{2+} adsorption (Fig. S3). In the wide-scan spectra (Fig. S3a), the Cd 3d peaks was only observed in nFe_2O_3@BC-Cd, indicating Cd^{2+} had been fixed on the surface of nFe_2O_3@BC-Cd after adsorption. Compared to nFe_2O_3@BC, the Na 1s at binding energy 1071.9 eV of nFe_2O_3@BC-Cd greatly decreased after Cd^{2+} adsorption (Fig. S3a, b, and c), confirming that ion exchange occurred during Cd adsorption (Zhang et al., 2016). In the C 1s XPS spectra of nFe_2O_3@BC (Fig. S3d), the peaks at 284.7, 286.6, and 288.7 eV can be assigned to C–C, C–O, and O═C–O, respectively; after Cd adsorption (Fig. S3e), the corresponding peaks of nFe_2O_3@BC-Cd slightly shifted to 284.8, 286.7, and 288.9 eV, respectively. This finding was consistent with the study of Zhang et al. (2020), they found the peaks of C–C, C–O, and O═C–O of $KMnO_4$ modified biochar were slightly shifted after Cd^{2+} adsorption. For the spectra of O 1s (Fig. S3f and g), the peaks of nFe_2O_3@BC and nFe_2O_3@BC-Cd at 530.3, 531.8, and 533.1 eV corresponded to Lattice-O, C═O/OH, and C–O. Notably, the relative content of C═O/OH in nFe_2O_3@BC-Cd decreased from 36.01% to 29.48% after Cd^{2+} adsorption (Table S3), which was due to complexation between C═O/OH and Cd^{2+}, generating inner-sphere complexes (Xu et al., 2019). By contrary, the relative C–O content of nFe_2O_3@BC-Cd increased from 46.66% to 54.76% after Cd^{2+} adsorption, which could be attributed to COO–Cd/O–Cd complex formation during adsorption (Zhu et al., 2020). Moreover, the relative C–O content of Lattice-O of nFe_2O_3@BC-Cd decreased by 9.06%. It was mainly ascribed to the loss of nFe_2O_3 in nFe_2O_3@BC during adsorption, and this explanation was also confirmed by results of section 3.7. In the spectra of Fe 2p (Fig. S3, h and i), the characteristic peaks of nFe_2O_3@BC and nFe_2O_3@BC-Cd were nearly unchanged. However, the content of Fe in nFe_2O_3@BC-Cd was decreased after adsorption (Fig. S3a and Table S3), suggesting the ion-exchange occurred between Fe ion and Cd^{2+} during adsorption (Yuan et al., 2020). In the spectra of Cd 3d (Fig. S3j), the binding energy of $3d_{3/2}$ and $3d_{5/2}$ were located at 412.4 and 405.7 eV, respectively, corresponding to Cd–O (Fig. S3j). It was owing to Cd^{2+} complexed with oxygen-containing functional groups on the surface of nFe_2O_3@BC, forming the –COO–Cd/-O-Cd; furthermore, nano-Fe_2O_3 particles could be hydrated during the adsorption process, generating Fe–OH groups then covered their surfaces; this surface oxide layer supplied surface sites to complex with Cd^{2+} and form Fe–O–Cd complexes (Li et al., 2019a; Zhu et al., 2020). Totally, Cd^{2+} could be adsorbed by nFe_2O_3@BC through complexation and ion exchange.

Although BC showed excellent reduction rates in Cd release (>99%), the release of Cd from sediment was not thoroughly eliminated. The Cd penetration into the BC capping layer was observed after 7 d at pH 3, 5, and 7 treatments. The release rate of Cd with BC capping increased significantly after 15 d, and it maintained a continuous release to the end. At pH 9 treatment, the Cd in overlying water kept a relatively stable state, indicating BC capping was suitable for *in situ* capping of Cd highly polluted sediments at pH 9 treatment. For nFe_2O_3@BC capping, the Cd releases were almost negligible in overlying water at all treatments during whole process, and their release trends reached a balance in the end. Significantly, Cd showed great biotoxicity to human body, and its recommendation standard value for drinking water introduced by World Health Organization (WHO) was only 3 μg/L (WHO, 2011). Based on the above results, nFe_2O_3@BC capping was recommended for *in situ* capping of Cd highly contaminated sediment all pH treatments.

Porewater plays a key role in the process of heavy metal exchange between sediment and overlying water (Tang et al., 2016). Hence, it is necessary to investigate the Cd variations in sediment porewater after capping. The Cd variations in porewater at different pH after capping are shown in Fig. 4. For 0–0.5 cm sediment porewater, Cd concentrations in the control at pH 3 treatment were 3.4, 4.3, and 9.8 times higher than

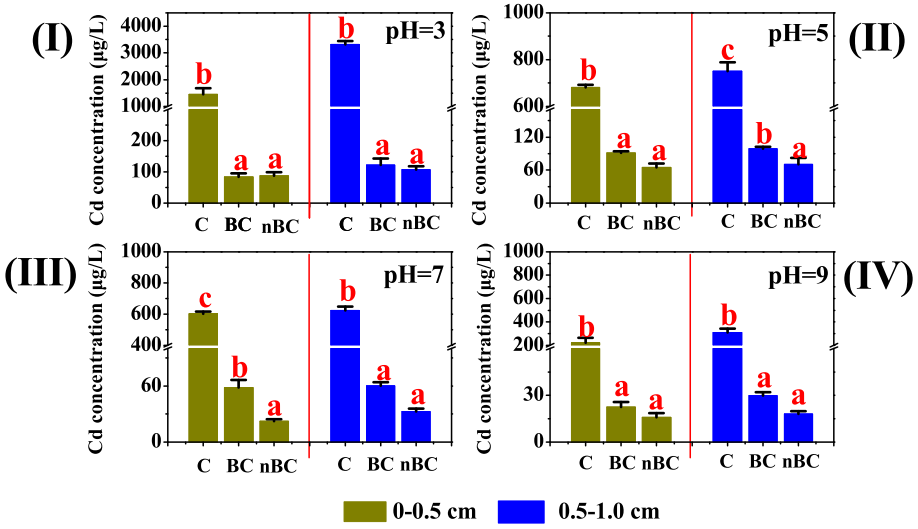

Fig. 4. Cd concentrations in porewater under different pH treatments after 60 d of capping (different letters (a, b, and c) on the bars denote significant differences among different groups ($P < 0.05$); nBC represents nFe_2O_3@BC)

those at pH 5, 7, and 9, respectively. Similar finding also presented at 0.5–1.0 cm porewater. This phenomenon demonstrated that Cd concentrations in porewater increased with pH decrease, which was line with Cd in overlying water. Compared to the control, the Cd concentrations in porewater in treated groups were significantly decreased after capping ($P < 0.05$), suggesting BC and nFe_2O_3@BC capping significantly inhibited the Cd release from sediment to porewater. As mentioned in section 3.2, the upper sediments were infiltrated by BC and nFe_2O_3@BC. Accordingly, the infiltration of BC and nFe_2O_3@BC could reduce Cd release from sediment to porewater via immobilization effect (Gao et al., 2020; Teng et al., 2020). Furthermore, BC and nFe_2O_3@BC capping could partly alleviate the influence of overlying water pH on sediment pH (Fig. 2), which was contributed to the decrease of Cd in porewater. After BC capping, the Cd concentration in porewater at pH 3 treatment was 8.54%, 78.59%, and 261.71% higher than those at pH 5, 7, and 9, respectively, showing Cd in porewater decreased with pH increase. The Cd variations in porewater with nFe_2O_3@BC capping were similar to BC capping. Cd concentrations in porewater with nFe_2O_3@BC capping were lower than those with BC capping, and significant decreases were found at pH 5 and 7 treatments ($P < 0.05$). This could be related to that the nFe_2O_3@BC possessed greater immobilization ability for mobile Cd in sediment compared to raw BC. For 0.5–1.0 cm porewater, the Cd concentrations at all pH treatments were lower than those in 0–0.5 cm section, especially for pH 3 treatment. This phenomenon was attributed to that upper sediment was more easily affected by pH and hydraulic disturbance. Totally, both BC and nFe_2O_3@BC inhibited the Cd release from sediments to porewater, and nFe_2O_3@BC was valid at all pH treatments.

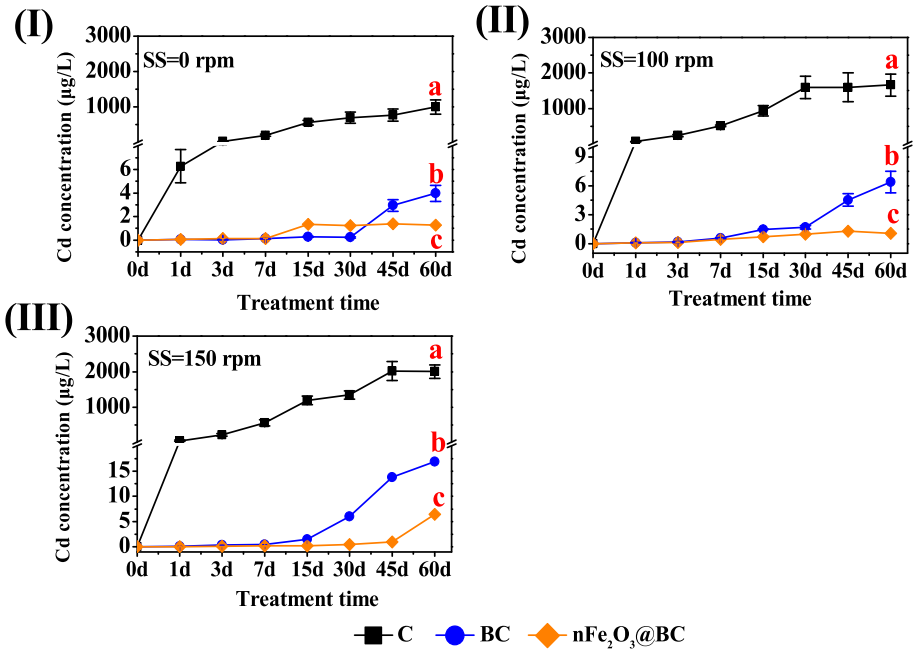

Fig. 5. Cd variations in overlying water under different stirring speeds with time (different letters (a, b, and c) on the bars denote significant differences among different groups ($P < 0.05$); nBC represents nFe_2O_3@BC)

3.4. The effects of disturbance intensity on Cd variations in overlying water and porewater

Water disturbance may promote desorption and/or release of heavy metals from sediment particles, posing potential threats to the aquatic ecosystem (Fremion et al., 2016; Pourabadehei and Mulligan, 2016). The Cd variations in overlying water under different SS treatments are illustrated in Fig. 5. Totally, the Cd concentrations in overlying water in controls increased with time during the entire capping process. At SS 150 rpm treatment, Cd increased by 21.1% and 162.3% compared to those at SS 0 and 100 rpm, respectively. This suggested that the release of Cd was promoted with the enhancement of disturbance intensity. During high disturbance, the molecular diffusion in the overlying water could change to the turbulent diffusion with the increase of disturbance intensity, and the diffusion intensity was greatly improved (Atkinson et al., 2007). Therefore, porewater, overlying water, and sediment were fully mixed, advancing the release of Cd from the sediment.

Under the three disturbance intensities, Cd concentrations in overlying water in the treated groups were all significantly lower than those in the controls ($P < 0.05$), and their reduction rates were >99% (Fig. S2b). However, the capping abilities of BC and nFe_2O_3@BC weakened with the increase of disturbance intensities. For example, after capping, the Cd concentration with BC capping at SS 150 rpm treatment was 1.6 and 3.3 times higher than those at SS 100 and 0 rpm, respectively. The reason maybe that high water disturbance could cause much lifting and floating of the upper capping materials, thus weakening the adsorption and fixation ability of BC and nFe_2O_3@BC capping to Cd^{2+}. Moreover, high water disturbance enhanced the diffusion rate of Cd^{2+}, which was also not conducive to the adsorption of Cd^{2+} by BC and nFe_2O_3@BC capping layers (Wang et al., 2020). Similarly, the Cd concentrations in overlying water with nFe_2O_3@BC capping were significantly lower than those with BC capping at all disturbance intensity treatments ($P < 0.05$). In detail, after incubation experiment, the Cd concentrations in overlying water with nFe_2O_3@BC capping at SS 0, 100, and 150 rpm were 5.0, 2.1, and 1.6 times lower than those with BC capping, respectively.

The Cd penetration into the BC capping layers all occurred on 7 d at all treatments. The release rate of Cd suddenly increased after 30 d at SS 0 rpm treatment, while similar phenomenon was observed after 15 d at SS 100 and 150 rpm. Furthermore, their release rates still increased until the end of the experiment. Thus, BC capping was inapplicable to cap Cd highly polluted sediment *in situ* at the three disturbance intensity treatments. For nFe_2O_3@BC capping, although Cd also penetrated the capping layer on 7 d at SS 0 and 100 rpm treatments, the Cd release maintained in a balance, presenting an effective capping. For SS 150 rpm treatment, the Cd penetration of capping layer was also found at 7 d. However, the Cd release was enhanced at 45 d and the release rate exhibited an increasing trend. This illustrated that nFe_2O_3@BC capping could effectively coverage Cd highly contaminated sediments *in situ* in still and weak disturbance waters, while it could be invalid in high disturbance water. The Cd concentrations in different section porewater under different SS treatments after 60 d capping are shown in Fig. S4. For 0–0.5 cm porewater, the Cd concentrations in porewater in controls were all significantly higher than those with BC and nFe_2O_3@BC capping ($P < 0.05$). Except for immobilization effect, the reduction in disturbance effect by capping was probably the cause of this phenomenon. Similar to different pH treatments, the Cd concentrations in porewater treated by BC capping were higher than those of nFe_2O_3@BC capping, especially for SS 100 rpm treatment. Moreover, the Cd concentrations in 0.5–1.0 cm porewater were also lower than those of 0–0.5 cm section.

3.5. The effects of capping on Cd in overlying water-sediment profile

For better comprehending the influences of BC and nFe_2O_3@BC capping on mobile Cd in sediment and the mechanisms for the interception of the internal Cd with BC and nFe_2O_3@BC capping, taking pH 7 treatment as an example, the vertical distribution of DGT-Cd concentrations along the sediment –overlying water profile was measured. The C_{DGT}-Cd variations in sediment – overlying water profile are presented in Fig. 6. In the control (Fig. 6a), the C_{DGT}-Cd concentrations were stable in the sediment profile. For the quartz sand layer, the C_{DGT}-Cd concentrations increased steadily with depth decrease. In the overlying water section, the C_{DGT}-Cd concentrations were also variable and showed great differences between different depths. Overall, C_{DGT}-Cd in different sections followed the order of overlying water > capping layer > sediment. This indicated that quartz sand layer failed to prevent the release of Cd from the sediment (Fig. 6a), and the Cd in the sediments has been immensely liberated into the overlying water.

Although the C_{DGT}-Cd variations in BC and nFe_2O_3@BC treatments were different from the control, C_{DGT}-Cd variations between BC and nFe_2O_3@BC treatments were similar. Their C_{DGT}-Cd concentrations all decreased continuously from deep to upper sediment, and then remained stable from capping layer to overlying water. The C_{DGT}-Cd concentrations in the sediments with BC and nFe_2O_3@BC capping were comparable to their capping layers. Compared to the control, the C_{DGT}-Cd concentrations in sediment with BC and nFe_2O_3@BC capping all were substantially lower. It confirmed that the mechanism in inhibiting Cd release with BC and nFe_2O_3@BC capping was not merely adsorption. This result was consistent with the study of Lin et al. (2020), who found using magnetic lanthanum/iron-modified bentonite capping greatly reduced the C_{DGT}-P concentration in sediment. Based on these results, another more important mechanism in inhibiting Cd release using BC and nFe_2O_3@BC capping was that capping could immensely reduce the Cd release from sediment to porewater. This potentially attributed to that capping reduced the adverse effect of overlying water pH and disturbance intensity on sediment due to their strong buffer and adsorption capacities.

3.6. Cd stability in BC and nFe_2O_3@BC capping layers after usage

Although capping layers could adsorb and store the released Cd from sediment, the changeable environment conditions probably affected the adsorbed Cd behavior in capping layer, resulting in potential secondary release risk. In order to assess the Cd stability in BC and nFe_2O_3@BC capping layers after their usage, the total concentrations and fraction distribution of Cd in BC and nFe_2O_3@BC capping layers in pH 7 treatments were recovered and determined after the capping experiment (Fig. 7). Generally, the mobility of heavy metal fractions presents F1 (acid-soluble fraction) > F2 (reducible fraction) > F3 (oxidizable fraction) > F4 (residual fraction) (Liu et al., 2018b), and the sum of F1, F2, and F3 can be considered as non-residual fraction, which is possible to

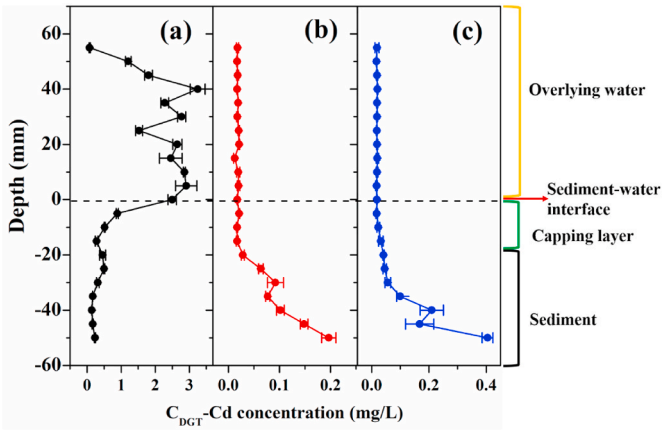

Fig. 6. The C_{DGT}-Cd in sediment-overlying water profile (a: control; b: BC capping; c: nFe_2O_3@BC capping).

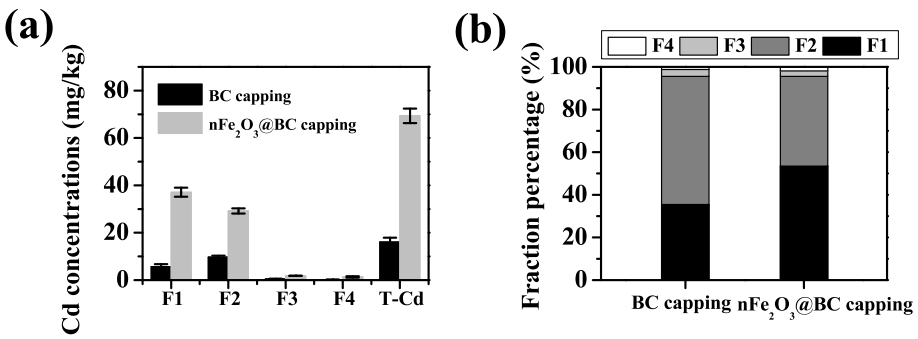

Fig. 7. Total Cd (a) and its fractions (b) in BC and nFe_2O_3@BC capping layers after 60 d of usage.

re-release once external environmental factor changes (such as pH and disturbance intensity) (Liu et al., 2020b). In this work, the concentrations of F1, F2, F3, and F4 in the BC capping layer were 5.70, 9.67, 0.51, and 0.20 mg/kg, respectively (Fig. 7a), accounting for 35.42%, 60.15%, 3.17%, and 1.26% of the total Cd, respectively. Obviously, the dominant fractions of Cd were F1 and F2. The non-residual fraction of Cd (F1 + F2 + F3) was 98.74%, indicating a high percentage of adsorbed Cd in BC capping layer was possible to re-release.

In Fig. 7b, the total adsorbed Cd concentration in the nFe_2O_3@BC capping layer was higher than that in BC (69.38 vs. 16.08 mg/kg). The concentrations of F1, F2, F3, and F4 in the nFe_2O_3@BC layer were 37.07, 29.21, 1.78, and 1.32 mg/kg, respectively, accounting for 53.43%, 42.10%, 2.57%, and 1.90% of the total Cd, respectively. Similar to BC, the non-residual fraction of Cd in the nFe_2O_3@BC capping layer also occupied for a high proportion (98.10%) of the total Cd. This demonstrated that nearly all adsorbed Cd in nFe_2O_3@BC capping layer was also potential to re-release. Consequently, for avoiding the secondary release of Cd in the capping layers, the further processing for the BC and nFe_2O_3@BC capping layers after Cd adsorption to attain a saturation state is necessary.

3.7. Fe dissolution risk in overlying water caused by capping

Although Fe showed minor biotoxicity compared to other toxic heavy metals (such as Pb and Cd), it would cause several aesthetic and operational troubles such as bad taste, discolouration, deposition in distribution systems resulting in aftergrowth and incidences of high turbidity (Sharma et al., 2005). Furthermore, lots of Fe dissolutions also could cause environment risk due to the release of associated heavy metals or production of oxyanions into soil solution and groundwater (Li et al., 2019a). Hence, the Fe dissolution risk in overlying water caused by capping should be evaluated. In this work, the total Fe concentrations in the overlying water at all treatments increased with decrease of pH and increase of disturbance intensities severally (Fig. 8). These phenomena could be explained that large amounts of H^+ accelerated the dissolution of iron oxides in sediment or nFe_2O_3@BC, leading to the release of dissolved Fe; moreover, the increase of disturbance intensity enhanced the release of Fe via turbulent diffusion. Overall, the Fe concentrations in the overlying water followed the order of nFe_2O_3@BC capping > control > BC capping. The concentrations of Fe in nFe_2O_3@BC capping were significantly higher than those in BC capping and the controls ($P < 0.05$). For example, the Fe concentration (pH 7 treatment) in the overlying water with nFe_2O_3@BC capping was 1.9 and 3.5 times higher than those of BC capping and the control, respectively. This indicated BC capping could inhibit the release of Fe from sediment, while nFe_2O_3@BC capping promoted the release of Fe.

The standard limit of total Fe concentration in surface drinking water source was lower than 0.3 mg/L based on the Environmental Quality Standards for Surface Water of China (GB 3838–2002) (SEPA, 2002). Evidently, the total Fe concentrations in overlying water with nFe_2O_3@BC capping in all treatments excessed the standard limit after capping. This result indicated that although nFe_2O_3@BC showed a high coverage efficiency on Cd polluted sediments, it could cause Fe dissolution risk, deteriorating water quality for drinking. Therefore, it is essential to comprehensively consider the environmental functions in the restoration area when the nFe_2O_3@BC was applied to cover Cd

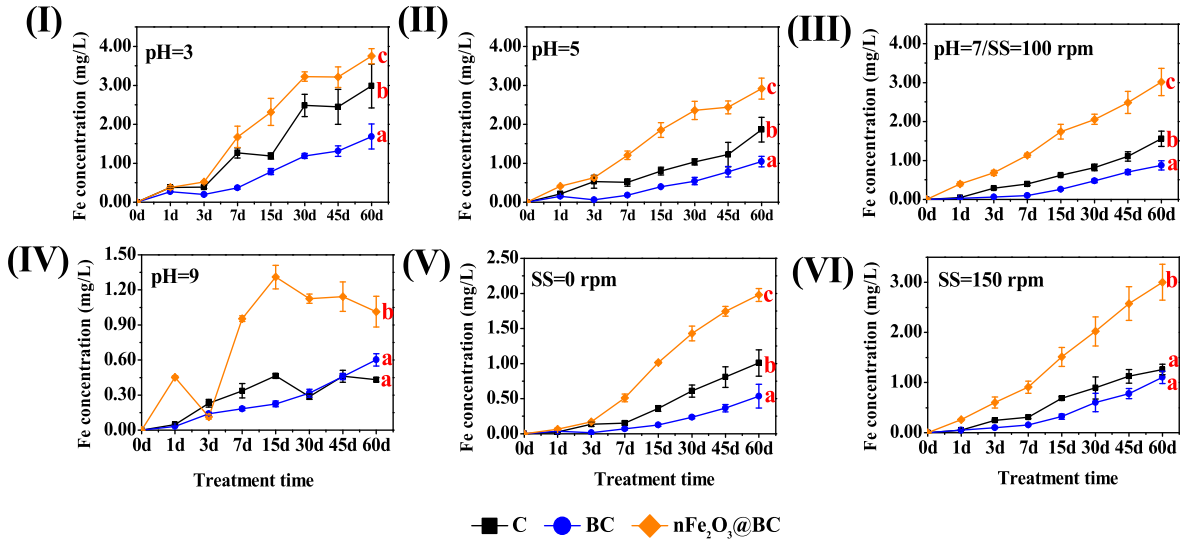

Fig. 8. The total Fe concentrations in overlying water under different pH and stirring speed with time (different letters (a, b, and c) on the bars denote significant differences among different groups ($P < 0.05$); nBC represents nFe_2O_3@BC)

contaminated sediment. However, except for Fe dissolution risk, it has been not clear whether BC and nFe_2O_3@BC capping will pose other adverse effects on overlying water quality based on the results of previous studies (Zhang et al., 2017; Zhu et al., 2019). Accordingly, the further analysis of other indicators (such as sense indicators and organic carbon) to measure overlying water quality when application of BC and nFe_2O_3@BC capping is also necessary in the next works.

4. Conclusions

The BC and nFe_2O_3@BC capping greatly restrained the release of Cd from sediment to overlying water and porewater, and nFe_2O_3@BC presented a better coverage efficiency compared to BC. Consideration of high toxicity of Cd, BC capping was inapplicable to remedy Cd highly polluted contaminated sediments in acidic and neutral water bodies, while nFe_2O_3@BC capping could stably inhibit Cd release in different pH treatments. Although BC and nFe_2O_3 capping could be invalid under high hydraulic disturbance, nFe_2O_3@BC capping could still work in low hydraulic disturbance. Based on DGT analysis, BC and nFe_2O_3@BC capping reduced Cd release from sediment to porewater. Excessive nFe_2O_3@BC capping could increase the risk of Fe release. The BC and nFe_2O_3@BC capping layers must be further processed in time due to the most adsorbed Cd in layers after usage was potential to re-release to water body. Notably, although application of nFe_2O_3@BC capping made Cd release keep a low and constant level in some treatments, the duration of balance state remains uncertain. Thus, it is deserved to further explore the term of validity of nFe_2O_3@BC capping, aiming to provide more valuable references for their practical applications in field remediation.

Declaration of competing interest

The authors declare that they have no known competing financial interests or personal relationships that could have appeared to influence the work reported in this paper.

Acknowledgements

This work was supported by the Key Project of Shandong Provincial Natural Science Foundation (Grant No.: ZR2020KE048) and the Strategic Priority Research Program of the Chinese Academy of Sciences (Grant No. XDA23050203). Additional support was from the Key Technology Research and Development Program of Shandong Province (Grant No. 2019GSF109002).

Appendix A. Supplementary data

Supplementary data to this article can be found online at https://doi.org/10.1016/j.envpol.2021.118134.

Credit author statement

Qunqun Liu: Investigation, Conceptualization, Writing – original draft, Writing – review & editing, Data curation, Formal analysis, Methodology. **Yanqing Sheng**: Methodology, Supervision, Project administration, Resources, Writing – review & editing. **Xiaozhu Liu**: Investigation, Methodology.

References

Ahmad, M., Lee, S.S., Rajapaksha, A.U., Vithanage, M., Zhang, M., Cho, J.S., Lee, S.E., Ok, Y.S., 2013. Trichloroethylene adsorption by pine needle biochars produced at various pyrolysis temperatures. Bioresour. Technol. 143, 615–622.

AQSIQ (General Administration of Quality Supervision, Inspection and Quarantine of the People's Republic of China) and SAC (Standardization Administration), 2009. Carbon Materials–Determination of the Ash Content (GB/T 1429-2009). Standards Press of China: Beijing, China. (In Chinese).

Atkinson, C.A., Jolley, D.F., Simpson, S.L., 2007. Effect of overlying water pH, dissolved oxygen, salinity and sediment disturbances on metal release and sequestration from metal contaminated marine sediments. Chemosphere 69, 1428–1437.

Chen, M., Ding, S., Gao, S., Fu, Z., Tang, W., Wu, Y., Gong, M., Wang, D., Wang, Y., 2019. Efficacy of dredging engineering as a means to remove heavy metals from lake sediments. Sci. Total Environ. 665, 181–190.

El-Naggar, A., Lee, M., Hur, J., Lee, Y.H., Igalavithana, A.D., Shaheen, S.M., Ryu, C., Rinklebe, J., Tsang, D.C.W., Ok, Y.S., 2020. Biochar-induced metal immobilization and soil biogeochemical process: an integrated mechanistic approach. Sci. Total Environ. 698, 134112.

Fremion, F., Courtin-Nomade, A., Bordas, F., Lenain, J.F., Juge, P., Kestens, T., Mourier, B., 2016. Impact of sediments resuspension on metal solubilization and water quality during recurrent reservoir sluicing management. Sci. Total Environ. 562, 201–215.

Gao, R., Hu, H., Fu, Q., Li, Z., Xing, Z., Ali, U., Zhu, J., Liu, Y., 2020. Remediation of Pb, Cd, and Cu contaminated soil by co-pyrolysis biochar derived from rape straw and orthophosphate: speciation transformation, risk evaluation and mechanism inquiry. Sci. Total Environ. 730, 139119.

Gu, B., Lee, C., Lee, T., Park, S., 2017. Evaluation of sediment capping with activated carbon and nonwoven fabric mat to interrupt nutrient release from lake sediments. Sci. Total Environ. 599–600, 413–421.

Huang, F., Gao, L.Y., Wu, R.R., Wang, H., Xiao, R.B., 2020. Qualitative and quantitative characterization of adsorption mechanisms for Cd^{2+} by silicon-rich biochar. Sci. Total Environ. 731, 139163.

Jin, X., Yu, C., Li, Y., Qi, Y., Yang, L., Zhao, G., Hu, H., 2011. Preparation of novel nano-adsorbent based on organic-inorganic hybrid and their adsorption for heavy metals and organic pollutants presented in water environment. J. Hazard Mater. 186, 1672–1680.

Li, B., Yin, W., Xu, M., Tan, X., Li, P., Gu, J., Chiang, P., Wu, J., 2019b. Facile modification of activated carbon with highly dispersed nano-sized α-Fe_2O_3 for enhanced removal of hexavalent chromium from aqueous solutions. Chemosphere 224, 220–227.

Lin, J., Zhao, Y., Zhan, Y., 2020. Control of internal phosphorus release from sediments using magnetic lanthanum/iron-modified bentonite as active capping material. Environ. Pollut. 264, 114809.

Liu, Q., Sheng, Y., Wang, W., Li, C., Zhao, G., 2020a. Remediation and its biological responses of Cd contaminated sediments using biochar and minerals with nanoscale zero-valent iron loading. Sci. Total Environ. 713, 136650.

Liu, Q., Sheng, Y., Wang, W., Liu, X., 2021. Efficacy and microbial responses of biochar-nanoscale zero-valent during *in-situ* remediation of Cd-contaminated sediment. J. Clean. Prod. 125076.

Liu, Q., Sheng, Y., Jiang, M., Zhao, G., Li, C., 2020b. Attempt of basin-scale sediment quality standard establishment for heavy metals in coastal rivers. Chemosphere 245, 125596.

Liu, Q., Wang, F., Meng, F., Jiang, L., Li, G., Zhou, R., 2018b. Assessment of metal contamination in estuarine surface sediments from Dongying City, China: use of a modified ecological risk index. Mar. Pollut. Bull. 126, 293–303.

Liu, S.J., Liu, Y.G., Tan, X.F., Zeng, G.M., Zhou, Y.H., Liu, S.B., Yin, Z.H., Jiang, L.H., Li, M.F., Wen, J., 2018a. The effect of several activated biochars on Cd immobilization and microbial community composition during in-situ remediation of heavy metal contaminated sediment. Chemosphere 208, 655–664.

Liu, W.F., Zhang, J., Zhang, C.L., Ren, L., 2012. Preparation and evaluation of activated carbon-based iron-containing adsorbents for enhanced Cr(VI) removal: mechanism study. Chem. Eng. J. 189, 295–302.

Li, X., Yang, Z., Zhang, C., Wei, J., Zhang, H., Li, Z., Ma, C., Wang, M., Chen, J., Hu, J., 2019a. Effects of different crystalline iron oxides on immobilization and bioavailability of Cd in contaminated sediment. Chem. Eng. J. 373, 307–317.

Li, X., Wang, C., Zhang, J., Liu, J., Liu, B., Chen, G., 2020. Preparation and application of magnetic biochar in water treatment: a critical review. Sci. Total Environ. 711, 134847.

Marrugo-Negrete, J., Pinedo-Hernández, J., Marrugo-Madrid, S., Díez, S., 2021. Assessment of trace element pollution and ecological risks in a river basin impacted by mining in Colombia. Environ. Sci. Pollut. Res. 28, 201–210.

MEPC (Ministry of Ecology and Environment of the People's Republic of China), 2017. Soil Quality-Determination of Cation Exchange Capacity- Hexamminecobalt Trichloride Solution-Spectrophotometric Method (HJ 889-2017). China Environmental Press, Beijing, China (In Chinese).

Peng, W., Li, X., Lin, M., Gui, H., Xiang, H., Zhao, Q., Fan, W., 2020. Biosafety of cadmium contaminated sediments after treated by indigenous sulfate reducing bacteria: based on biotic experiments and DGT technique. J. Hazard Mater. 384, 121439.

Pourabadehei, M., Mulligan, C.N., 2016. Resuspension of sediment, a new approach for remediation of contaminated sediment. Environ. Pollut. 273, 63–75.

Raymond, C., Samuelsson, G.S., Agrenius, S., Schaanning, M.T., Gunarsson, J.S., 2021. Impaired benthic macrofauna function 4 years after sediment capping with activated carbon in the Grenland fjords, Norway. Environ. Sci. Pollut. Res. 28, 16181–16197.

SEPA (State Environmental Protection Administration), 2002. Environmental Quality Standards for Surface Water (GB 3838-2002). China Environmental Press, Beijing, China (In Chinese).

Sharma, S.K., Petrusevski, B., Schippers, J.C., 2005. Biological iron removal from groundwater: a review. J. Water Supply Res. Technol. - Aqua 54, 239–246.

Song, J., Liu, Q., Sheng, Y., 2019. Distribution and risk assessment of trace metals in riverine surface sediments in gold mining area. Environ. Monit. Assess. 191, 191.

Taneez, M., Hurel, C., Mady, F., Francour, P., 2018. Capping of marine sediments with valuable industrial by-products: evaluation of inorganic pollutants immobilization. Environ. Pollut. 239, 714–721.

Tang, W., Duan, S., Shan, B., Zhang, H., Zhang, W., Zhao, Y., Zhang, C., 2016. Concentrations, diffusive fluxes and toxicity of heavy metals in pore water of the Fuyang River, Haihe Basin. Ecotoxicol. Environ. Saf. 127, 80–86.
Teng, F., Zhang, Y., Wang, D., Shen, M., Hu, D., 2020. Iron-modified rice husk hydrochar and its immobilization effect for Pb and Sb in contaminated soil. J. Hazard Mater. 398, 122977.
Wang, H., Cai, J., Liao, Z., Jawad, A., Chen, Z., 2020. Black liquor as biomass feedstock to prepare zero-valent iron embedded biochar with red mud for Cr(VI) removal: mechanisms insights and engineering practicality. Bioresour. Technol. 311, 123553.
Wang, Y., Ding, S., Gong, M., Xu, S., Xu, W., Zhang, C., 2016. Diffusion characteristics of agarose hydrogel used in diffusive gradients in thin films for measurements of cations and anions. Anal. Chim. Acta 945, 47–56.
Wang, L., Chen, S.S., Sun, Y., Tsang, D.C., Yip, A.C., Ding, S., Hou, D., Baek, K., Ok, Y.S., 2019. Efficacy and limitations of low-cost adsorbents for in-situ stabilisation of contaminated marine sediment. J. Clean. Prod. 212, 420–427.
Wan, J., Zeng, G., Huang, D., Hu, L., Xu, P., Huang, C., Deng, R., Xue, W., Lai, C., Zhou, C., Zheng, K., Ren, X., Gong, X., 2018. Rhamnolipid stabilized nano-chlorapatite: synthesis and enhancement effect on Pb-and Cd-immobilization in polluted sediment. J. Hazard Mater. 343, 332–339.
World Health Organization (WHO), 2011. Guidelines for Drinking Water Quality, fourth ed. Geneva.
Xiao, L., Feng, L., Yuan, G., Wei, J., 2020. Low-cost field production of biochars and their properties. Environ. Geochem. Health 42, 1569–1578.
Xiong, C., Wang, D., Tam, N.F., Dai, Y., Zhang, X., Tang, X., Yang, Y., 2018. Enhancement of active thin-layer capping with natural zeolite to simultaneously inhibit nutrient and heavy metal release from sediments. Ecol. Eng. 119, 64–72.
Xue, W., Huang, D., Zeng, G., Wan, J., Zhang, C., Xu, R., Cheng, M., Deng, R., 2018. Nanoscale zero-valent iron coated with rhamnolipid as an effective stabilizer for immobilization of Cd and Pb in river sediments. J. Hazard Mater. 341, 381–389.
Xu, H., Yuan, H., Yu, J., Lin, S., 2019. Study on the competitive adsorption and correlational mechanism for heavy metal ions using the carboxylated magnetic iron oxide nanoparticles (MNPs-COOH) as efficient adsorbents. Appl. Surf. Sci. 473, 960–966.
Yang, F., Zhang, S., Sun, Y., Cheng, K., Li, J., Tsang, D.C., 2018. Fabrication and characterization of hydrophilic corn stalk biochar-supported nanoscale zero-valent iron composites for efficient metal removal. Bioresour. Technol. 265, 490–497.
Yang, X., Pan, H., Shaheen, S.M., Wang, H., Rinklebe, J., 2021. Immobilization of cadmium and lead using phosphorus-rich animal-derived and iron-modified plant-derived biochars under dynamic redox conditions in a paddy soil. Environ. Int. 156, 106628.
Yin, H., Kong, M., 2015. Reduction of sediment internal P-loading from eutrophic lakes using thermally modified calcium-rich attapulgite-based thin-layer cap. J. Environ. Manag. 151, 178–185.
Yin, H., Yang, C., Yang, P., Kaksonen, A.H., Douglas, G.B., 2021. Contrasting effects and mode of dredging and in situ adsorbent amendment for the control of sediment internal phosphorus loading in eutrophic lakes. Water Res. 189, 116644.
Yuan, S., Hong, M., Li, H., Ye, Z., Gong, H., Zhang, J., Huang, Q., Tan, Z., 2020. Contributions and mechanisms of components in modified biochar to adsorb cadmium in aqueous solution. Sci. Total Environ. 773, 139320.
Yu, Y., Chen, P.J., 2015. Key factors for optimum performance in phosphate removal from contaminated water by a Fe-Mg-La tri-metal composite sorbent. J. Colloid Interface Sci. 445, 303–311.
Zhang, J., Ma, X., Lei, Y., Zhou, D., 2020. Comparison of adsorption behavior studies of Cd^{2+} by vermicompost biochar and $KMnO_4$-modifed vermicompost biochar. J. Environ. Manag. 256, 109959.
Zhang, S., Tian, K., Jiang, S., Jiang, H., 2017. Preventing the release of Cu^{2+} and 4-CP from contaminated sediments by employing a biochar capping treatment. Ind. Eng. Chem. Res. 56, 7730–7738.
Zhang, C., Yu, Z., Zeng, G., Huang, B., Dong, H., Huang, J., Yang, Z., Wei, J., Hu, L., Zhang, Q., 2016. Phase transformation of crystalline iron oxides and their adsorption abilities for Pb and Cd. Chem. Eng. J. 284, 247–259.
Zhao, Q., Li, X., Xiao, S., Peng, W., Fan, W., 2021. Integrated remediation of sulfate reducing bacteria and nano zero valent iron on cadmium contaminated sediments. J. Hazard Mater. 406, 124680.
Zhu, L., Tong, L., Zhao, N., Wang, X., Yang, X., Lv, Y., 2020. Key factors and microscopic mechanisms controlling adsorption of cadmium by surface oxidized and aminated biochars. J. Hazard Mater. 382, 121002.
Zhu, Y., Shan, B., Huang, J., Teasdale, P.R., Tang, W., 2019. *In situ* biochar capping is feasible to control ammonia nitrogen release from sediments evaluated by DGT. Chem. Eng. J. 374, 811–821.